Electronic structure of (001) $(AlAs)_k(GaAs)_l(AlAs)_m(GaAs)_n$ superlattices

1996 J. Phys.: Condens. Matter 8 8859

(http://iopscience.iop.org/0953-8984/8/45/019)

J. Phys.: Condens. Matter **8** (1996) 8859–8867. Printed in the UK

Electronic structure of (001) $(AlAs)_k(GaAs)_l(AlAs)_m(GaAs)_n$ superlattices

L Fernández-Alvarez†, G Monsivais‡ and V R Velasco§

† Instituto de Ciencia de Materiales, CSIC, Cantoblanco, 28049 Madrid, Spain
‡ Instituto de Física, UNAM, Apartado Postal 20-364, 01000 México, DF, Mexico
§ Instituto de Ciencia de Materiales, CSIC, Cantoblanco, 28049 Madrid, Spain

Received 9 April 1996, in final form 20 August 1996

Abstract. The electronic structure of (001) $(AlAs)_k(GaAs)_l(AlAs)_m(GaAs)_n$ superlattices is studied for many combinations of values of k, l, m and n. We have charted the regions of indirect gap and direct gap respectively by studying energy eigenvalues, especially band-edge levels, and also the spatial dependence of the local amplitude of some representative states, in order to obtain information on the confinement problems. The calculations are based on an sp^3s^* empirical tight-binding model and on the surface Green-function-matching method.

1. Introduction

Over the last few years there has been a continued interest in the properties and device applications of semiconductor superlattices [1]. The developments achieved in growth techniques and microfabrication technology have made it possible to control the structure, composition and doping of semiconductor heterostructures to a very high precision. In this way more complicated heterostructures than the simple quantum wells and binary superlattices have appeared in recent years. Some of these heterostructures, such as the digital quantum wells [2, 3], have more than two non-equivalent interfaces. The idea behind the fabrication of these heterostructures is the design of systems having electronic band structures which exhibit the desired optical and transport properties for some specific application [4]. This was usually done by changing the layer widths in quantum wells and superlattices or by introducing new materials or changing the doping. All of these approaches have their limitations, because of difficulties in the actual growth processes, the diffusion of impurities, etc.

Some years ago alternative methods for modulating the superlattice minibands were proposed [5, 6]. In those cases the idea was to introduce spatially localized defects (δ-doping) periodically repeated in the well layers and/or in the barrier layers of the superlattices. In practice it is not easy to achieve the desired band structure and material properties by controlling the position and concentration of the dopants, without encountering some of the difficulties and problems mentioned above. A different approach was recently proposed in which the modulation of the superlattice minibands was achieved by considering superlattices with a two-well period [7]. In this way it is possible to avoid the difficulties already discussed and to take advantage of using those systems in which the growth of heterostructures is easier and better controlled. All of these and other similar cases have been studied by using the effective-mass approximation [5–10].

0953-8984/96/458859+09$19.50

It is clear that a very good candidate for this kind of modulation is the AlAs–GaAs system. This is a very well known system which exhibits excellent growth characteristics and provides a very good starting point for this kind of system. We shall study the electronic properties of (001) $(AlAs)_k(GaAs)_l(AlAs)_m(GaAs)_n$ superlattices, where k, l, m, n indicate the numbers of principal layers in each one of the different slabs forming the superlattice period. In this way we have superlattices with alternating barriers formed by k and m principal layers of AlAs and wells formed by l and n principal layers of GaAs. We shall employ an sp^3s^* empirical tight-binding (ETB) Hamiltonian [11] including spin–orbit coupling [12] which has given good results in the study of the AlAs–GaAs binary superlattices [13]. We shall study this system here and analyse the influence of the variation of the thicknesses of the constituent slabs on the electronic properties of these superlattices.

To study this type of superlattice in which we have *four* non-equivalent interfaces we shall employ a recent extension of the surface Green-function-matching (SGFM) method [14], which provides for a compact way of studying systems with an arbitrary number, N, of non-equivalent interfaces [15]. We shall obtain the eigenvalues of the lowest conduction bands and highest valence bands, as well as their spatial localization in order to obtain information on the confinement of the different states.

In section 2 we present the theoretical model employed in our calculations, together with the basic SGFM formulas needed for the analysis. Results are presented in section 3, while the conclusions are presented in section 4.

2. The model and method

In order to study semiconductor heterostructures several theoretical approaches can be used. *Ab initio* methods have been used to study short-period superlattices [16–20]. These methods are quite demanding as regards memory and computer time resources. Because of this, a useful alternative for the study of the electronic properties of heterostructures having long periods or thicknesses is provided by semiempirical methods like the $\boldsymbol{k}\cdot\boldsymbol{p}$ method [21] and the empirical tight-binding (ETB) Hamiltonians [22]. The ETB models include the multiband and band-mixing characteristics together with the crystalline symmetry for the bulk constituent materials, and they can be more useful than the $\boldsymbol{k}\cdot\boldsymbol{p}$ method in the study of the properties of these systems in the complete Brillouin zone. It is also known that self-consistent ETB calculations for semiconductor interfaces [23–25] gave results for the band offset comparable to those obtained using the local density approximation (LDA) [26]. It was then quite natural to employ ETB Hamiltonians to study the electronic properties of heterostructures. It has been found that the electronic properties thus obtained [13, 20, 27] are in qualitative agreement with those obtained from *ab initio* calculations [16–20]. Even the quantitative agreement for properties like the gaps in the band structure are in the range 0.1 eV [13, 17, 18] to 0.02 eV [20]. It is then clear that the ETB Hamiltonians provide a very efficient and reasonable way to study the electronic properties of long-period heterostructures, with a lower cost in computer resources.

We use here an ETB sp^3s^* model with the parameters corrected according to reference [28] to include the spin–orbit coupling. We have used the following energy reference: $E_V(\mathrm{AlAs}) = 0$ eV, $E_C(\mathrm{AlAs}) = 2.30$ eV, which corresponds to the AlAs indirect band gap; $E_V(\mathrm{GaAs}) = 0.55$ eV and $E_C(\mathrm{GaAs}) = 2.10$ eV. This band offset is within experimentally accepted values for (001) interfaces [29] and corresponds to a 66/34 band-offset rule [30]. The ETB parameters employed in our calculations are those of [31]. They take into account the spin–orbit coupling and thus they are different from those of reference [11]. This parametrization gives effective masses for the conduction electrons at the Γ point of

$m^* = 0.106$ for GaAs and $m^* = 0.249$ for AlAs, which are higher than those measured experimentally, $m^* = 0.065$ for GaAs and $m^* = 0.19$ for AlAs. In spite of this the parametrization has given good results when compared with experimental data in the case of (311) AlAs/GaAs superlattices [32, 33], and triangular [34], inverse parabolic [35] and digital quantum wells [36]. We could improve on the effective masses of the conduction electrons by using a Hamiltonian including interactions up to second neighbours. We would then have more parameters at our disposal and it would then be possible to improve on the results obtained with the simpler Hamiltonian. It would also be possible to use different parametrization schemes to fit the effective masses [37, 38]. This would affect some details concerning the thicknesses of the layers where the different localizations appear, and the numerical values of the different energy levels, but it would not modify the overall qualitative picture emerging from the calculations. For all of these reasons we decided to keep the simpler parametrization in order to obtain the general picture.

We shall now study the electronic properties of (001) $(AlAs)_k(GaAs)_l(AlAs)_m(GaAs)_n$ superlattices. We shall employ a recently developed version of the SGFM method to deal with systems having an arbitrary number, N, of non-equivalent interfaces [15]. In our case $N = 4$. The method has been fully explained elsewhere and need not be repeated here. The eigenvalues are obtained from the peaks in the imaginary part of the trace of the interface projection of the Green function of the matched system $\tilde{\boldsymbol{G}}_S^{-1}$ [15]. A small imaginary part of 10^{-3} eV was added to the real energy variable, which was varied by steps of 0.01 eV, and iterations were carried out until absolute differences between the last iterations of order 10^{-6} eV were obtained. We have found in previous practical calculations that this provides a satisfactorily accurate procedure. The spatial localization was obtained by calculation of the local density of states at the different layers of the superlattice period, which is directly obtained from the Green function of the whole system $\boldsymbol{G}_S$ [15]. We have concentrated on the lowest conduction and highest valence states, which are the most important for the electro-optic properties of the heterostructures, and we have studied the high-symmetry Γ and X points only.

3. Results

In the case of (001) $(AlAs)_n(GaAs)_m$ superlattices it was found [13] that these superlattices show a great variety of electronic structures. The top of the valence band is always confined to the GaAs slabs, but the bottom of the conduction band shows different behaviours. Folding effects induced the appearance of a region in the (n, m) chart where comparable amplitudes were found for the two constituents. *Four* distinct types were found, only one exhibiting an indirect gap in the Brillouin zone of the superlattice, covering the range $(n \leqslant 5, m \leqslant 6)$.

In order to see the differences introduced by the two-well superlattices $(AlAs)_k(GaAs)_l(AlAs)_m(GaAs)_n$ we have covered the range $(2 \leqslant k, l, m, n \leqslant 8)$ which spans basically the range of direct- and indirect-gap superlattices found in the binary case, without covering the high numbers which give direct-gap superlattices. In figure 1 we present the basic conclusions of our calculations. In order to present the results it is convenient to convert the index pairs (k, l) and (m, n) to a new index j, in such a way that we can label the superlattice (k, l, m, n) as (j, j') in the new indexing system. It is clear that there are different ways to perform this relabelling. We have chosen the following

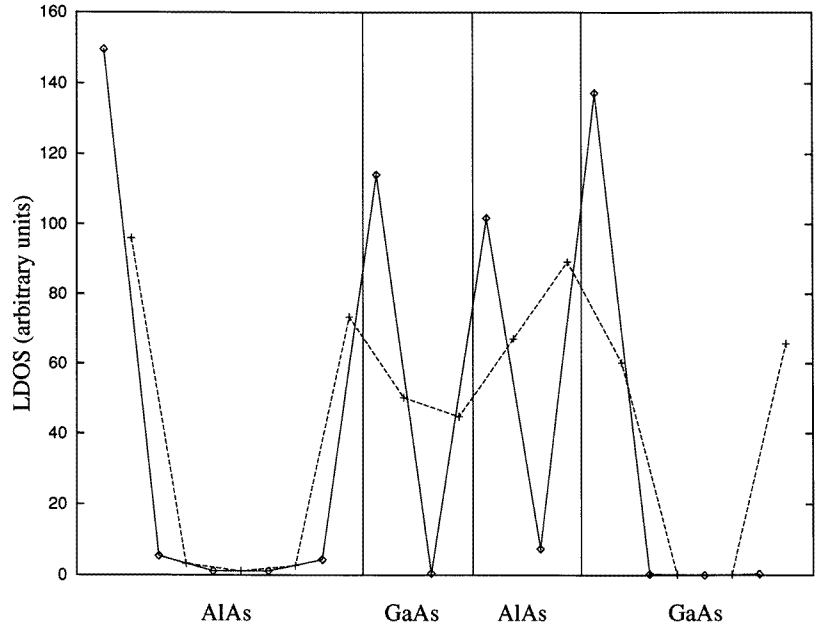

(a)

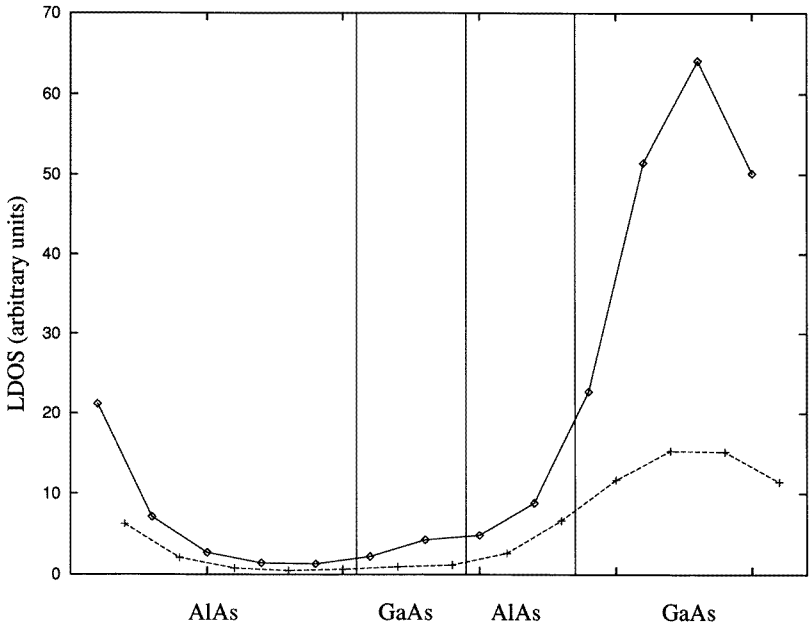

(b)

Figure 1. The local density of states, in arbitrary units, of some selected states of the (5, 2, 2, 4) superlattice. (a) The conduction band bottom at the in-plane X point. (b) The valence band top at the Γ point. (c) The second valence band at the Γ point. (d) The third valence band at the Γ point. The figure displays the spatial distribution in the different atomic layers of the superlattice. A solid line represents cation layers and a dashed line represents anion layers.

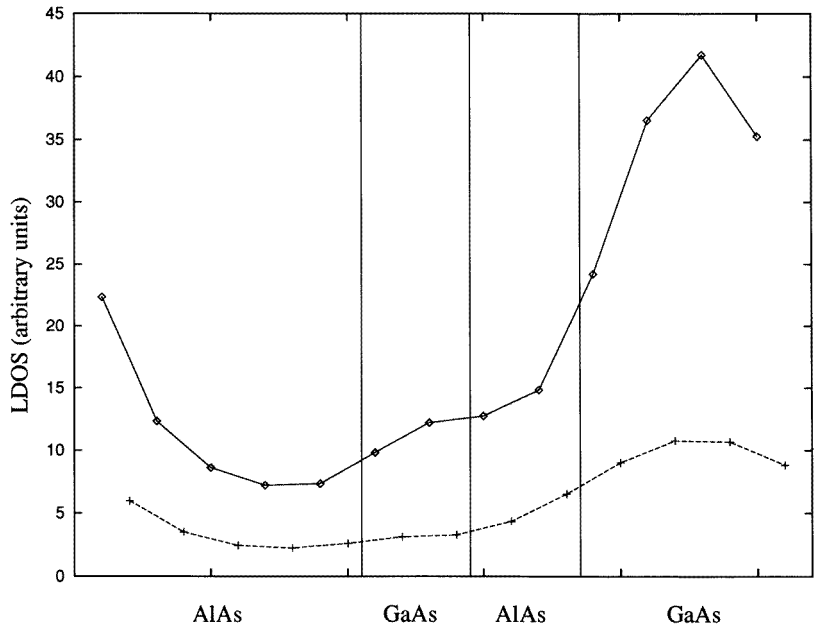

(c)

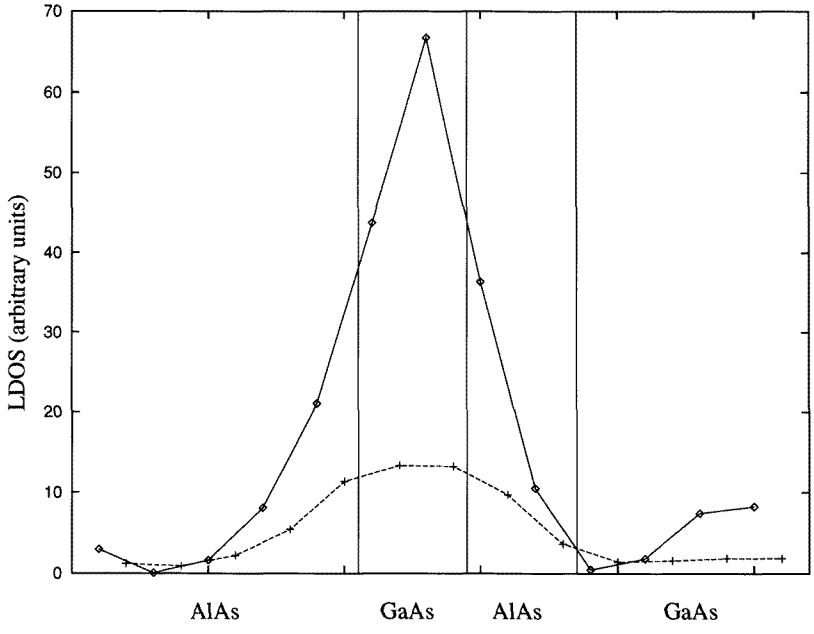

(d)

Figure 1. (Continued)

assignment:

(k, l)	(2, 2)	(2, 3)	(3, 2)	(4, 2)	(3, 3)	(2, 4)	(2, 5)	(3, 4)	(4, 3)	(5, 2)
j	1	2	3	4	5	6	7	8	9	10

Table 1. Each (n, m) entry gives the corresponding values in eV of X_c, Γ_c, Γ_{hh} and Γ_{lh}, from top to bottom.

	1	2	3	4	5	6	7	8	9	10
1	2.285 2.335 0.193 0.185									
2	2.285 2.342 0.256 0.236	2.286 2.351 0.286 0.269								
3	2.285 2.318 0.179 0.169	2.286 2.321 0.244 0.219	2.285 2.318 0.166 0.156							
4	2.285 2.305 0.169 0.157	2.286 2.304 0.237 0.207	2.285 2.303 0.157 0.145	2.285 2.302 0.148 0.136						
5	2.285 2.321 0.244 0.219	2.286 2.323 0.273 0.252	2.285 2.317 0.234 0.205	2.285 2.305 0.228 0.195	2.286 2.324 0.260 0.236					
6	2.285 2.341 0.316 0.281	2.286 2.325 0.328 0.302	2.285 2.320 0.309 0.267	2.285 2.305 0.305 0.256	2.286 2.323 0.318 0.286	2.286 2.305 0.348 0.325				
7	2.285 2.312 0.365 0.320	2.286 2.298 0.369 0.333	2.285 2.320 0.360 0.307	2.285 2.304 0.358 0.298	2.286 2.319 0.363 0.319	2.286 2.284 0.377 0.348	2.286 2.270 0.391 0.364			
8	2.285 2.320 0.309 0.267	2.286 2.323 0.318 0.286	2.285 2.319 0.304 0.254	2.285 2.305 0.301 0.245	2.286 2.323 0.309 0.272	2.286 2.323 0.338 0.309	2.286 2.306 0.369 0.334	2.286 2.324 0.327 0.294		
9	2.285 2.304 0.237 0.207	2.286 2.305 0.265 0.239	2.285 2.305 0.228 0.195	2.285 2.304 0.223 0.185	2.286 2.305 0.252 0.225	2.286 2.305 0.313 0.275	2.286 2.304 0.361 0.309	2.286 2.305 0.305 0.261	2.286 2.302 0.243 0.214	
10	2.285 2.295 0.163 0.148	2.286 2.296 0.233 0.198	2.285 2.296 0.151 0.137	2.285 2.295 0.143 0.129	2.286 2.296 0.225 0.187	2.286 2.296 0.303 0.248	2.286 2.296 0.357 0.292	2.286 2.296 0.300 0.239	2.286 2.295 0.221 0.178	2.285 2.292 0.137 0.122

and so on (we proceed in a similar way for (m, n)). It is easy to see that we are following the diagonals in a zigzag way.

Table 1 gives the values of the two topmost states of the valence band at the Γ point, corresponding to a heavy-hole (Γ_{hh}), and a light-hole (Γ_{lh}) state, respectively, and the

bottom of the conduction bands at the Γ and X points (Γ_c and X_c, respectively). The superlattice gap is indirect when the bottom of the conduction band is at the in-plane X point of the superlattice Brillouin zone. The superlattice gap is *fully* direct when the bottom of the conduction band is at the Γ point of the superlattice Brillouin zone and its amplitude is confined to the GaAs slabs, as in the binary-superlattice cases. It is easy to see that the number of possible combinations for obtaining indirect-gap superlattices has increased considerably in the present case.

We shall show now briefly consider the richer variety of behaviour exhibited by the spatial localization of the different states.

In order to show this we shall consider the (5, 2, 2, 4) superlattice which is the (10, 6) one according to the new labels, and a fully indirect-gap superlattice as indicated in table 1. Figure 1(a) gives the local density of states for the bottom of the conduction band at the in-plane X point of the superlattice Brillouin zone. It can now be seen that there is not a clear spatial localization in this case. The state has mixed orbital character with predominant p_z and s^* contributions. The mixed localization in the present case can be understood if we take into account that the (5, 2) and (2, 4) binary superlattices have their spectral strength distributed over the whole period of the superlattice, although with more intensity in the AlAs layers. It is clear that the (5, 2, 2, 4) superlattice can also be considered as a combination of the (2, 2) and (4, 5) binary superlattices. In these binary superlattices the spectral strength presents the same behaviour as discussed before. The fact of now having the two monolayers of GaAs contiguous to the two monolayers of AlAs produces a stronger localization in these layers, and enhances the localization at the anion interface layers. Figure 1(b) gives the local density of states corresponding to the top of the valence band at the Γ point. In this case there is a strong localization in only one of the GaAs slabs. The state has $p_x = p_y$ contributions, thus corresponding to a heavy-hole state. Figure 1(c) gives the same information for the second valence band state. It provides evidence of the same localization, and it has $p_x = p_y < p_z$ contributions, thus corresponding to a light-hole state. Figure 1(d) gives the same information for the third valence band state. This state is also localized in only one GaAs slab, but in this case in that having two monolayers. It has $p_x = p_y$ contributions, thus corresponding to a heavy-hole state. This selective localization constitutes a difference as regards the behaviour of the local density of states exhibited by other fully indirect-gap superlattices, like the (3, 4, 2, 4) one, or (8, 6) according to the relabelling explained before, which have localization at both GaAs slabs for the highest valence bands.

In the case of the direct-gap superlattices we have found that the lowest conduction and highest valence bands at the Γ point of the superlattice exhibit localization at the GaAs slabs. The lowest conduction band has predominantly s character and the dominant contribution comes from the cations.

The local density of states can help us to understand the experimentally observed transitions, by looking to the localizations of the different states, and estimating the contributions of the overlaps of the different states [39].

We have seen that the two-well (AlAs)/(GaAs) superlattices have more possibilities of combining to give indirect superlattices, and that when one combines a direct superlattice with an indirect one, there is a high probability of ending up with an indirect two-well superlattice. We have also seen that they exhibit a richer variety in the behaviour of the spatial localization for the different states. It is also possible to obtain selective localization in only one slab, and this slab can be different for the different states of a given superlattice.

4. Conclusions

We have studied the electronic properties of (AlAs)/(GaAs) two-well (001) superlattices. We have considered all of the possible combinations for superlattices in which the thickness of the different slabs forming the superlattice period is varied between two and eight monolayers. We have found that the top of the valence band is always at the superlattice Γ point, and that the highest valence band states are localized in the GaAs slabs of the superlattice, although in some cases the state can be localized in only one of the constituent GaAs slabs. We have found that the highest valence band states of a given superlattice can be localized selectively in each one of the GaAs slabs forming the superlattice. All of these states can be classified according to the heavy- and light-hole scheme.

For the bottom of the conduction band we have found that in the majority of the superlattices considered it corresponds to the in-plane X point of the superlattice Brillouin zone, thus producing indirect-gap superlattices. In these cases the spatial localization is in the AlAs slabs of the superlattice, although in some cases there is contribution to the local density of states in all of the slabs of the superlattice. In these indirect superlattices the orbital character of the bottom conduction band is a mixed one, although with predominant p_z and s^* contributions. We have found a small number of superlattices in which the bottom of the conduction band at the Γ point is lower than that at the in-plane X point, and in these cases the states show a spatial localization in the GaAs slabs forming the superlattice and have s-orbital character. It is clear that these $(AlAs)_k(GaAs)_l(AlAs)_m(GaAs)_n$ superlattices can show competing effects of the $(AlAs)_k(GaAs)_l$ and $(AlAs)_m(GaAs)_n$ superlattices, but also of the $(GaAs)_l(AlAs)_m$ and $(GaAs)_n(AlAs)_k$ ones. This opens the door to a very rich variety of spatial localizations, from which we have shown only a few cases.

It is then clear that the two-well (AlAs)(GaAs) superlattices provide the possibility, because of the easy growth possibilities, of a very rich variety of superlattices with different spatial localizations and also a larger number of superlattices with indirect gaps.

Acknowledgments

We are grateful to Professor F García-Moliner for his helpful advice and the critical reading of the manuscript. This work was partially supported by the Spanish DGICYT through Grant No PB93-1251. LF-A thanks the Spanish Ministry of Education and Science for support. GM thanks the European Community for support through Contract No CI1*-CT93-0225.

References

[1] Vinter B and Weisbuch C 1991 *Quantum Semiconductor Structures* (San Diego, CA: Academic)
[2] Capasso F, Cox H M, Hutchinson A L, Olsson N A and Hummel S G 1984 *Appl. Phys. Lett.* **45** 1193
[3] Sundaram M, Wixforth A, Geels R S, Gossard A C and English J H 1991 *J. Vac. Sci. Technol.* B **9** 1524
[4] Capasso F 1987 *Science* **235** 172
[5] Beltram F and Capasso F 1988 *Phys. Rev.* B **38** 3580
[6] Ihm G, Noh S K, Lee J H, Hwang J-S and Kim T W 1991 *Phys. Rev.* B **44** 6266
[7] Ihm G, Noh S K, Lee J H, Lee S J and Kim T W 1992 *Superlatt. Microstruct.* **12** 155
[8] Jiang H X and Lin J Y 1986 *Phys. Rev.* B **33** 5851
[9] Jiang H X and Lin J Y 1987 *Am. J. Phys.* **55** 462
[10] Shi J and Pan S 1993 *Superlatt. Microstruct.* **13** 413
[11] Vogl P, Hjalmarson H P and Dow J D 1983 *J. Phys. Chem. Solids* **44** 365
[12] Chadi D J 1977 *Phys. Rev.* B **16** 790
[13] Muñoz M C, Velasco V R and García-Moliner F 1989 *Phys. Rev.* B **39** 1786

[14] García-Moliner F and Velasco V R 1992 *Theory of Single and Multiple Interfaces* (Singapore: World Scientific)
[15] Fernández-Alvarez L, Monsivais G, Vlaev S and Velasco V R 1996 *Surf. Sci.* to be published
[16] Wood D M, Wei S-H and Zunger A 1988 *Phys. Rev.* B **37** 1342
[17] Alouani M, Gopalan S, Garriga M and Christensen N E 1988 *Phys. Rev. Lett.* **61** 1643
[18] Gopalan S, Christensen N E and Cardona M 1989 *Phys. Rev.* B **39** 5165
[19] Dandrea R G and Zunger A 1991 *Phys. Rev.* B **43** 8962
[20] Willatzen M, Lew Yan Voon L C, Santos P V, Cardona M, Munzar D and Christensen N E 1995 *Phys. Rev.* B **52** 5070
[21] Kane E O 1966 *Semiconductors and Semimetals* vol 1, ed R K Willardson and A C Beer (New York: Academic) p 75
[22] Slater J C and Koster G F 1954 *Phys. Rev.* **94** 1498
[23] Muñoz A, Sánchez-Dehesa J and Flores F 1987 *Phys. Rev.* B **35** 6468
[24] Haussy B, Priester C, Allan G and Lannoo M 1987 *Phys. Rev.* B **36** 1105
[25] Flores F, Durán J C and Muñoz A 1987 *Phys. Scr.* T **19** 102
[26] Van de Walle C G and Martin R M 1986 *J. Vac. Sci. Technol.* B **4** 1055
[27] Schulman J N and McGill T C 1979 *Phys. Rev.* B **19** 6341
[28] Priester C, Allan G and Lannoo M 1988 *Phys. Rev.* B **37** 8519
[29] Fu Y and Chao K A 1991 *Phys. Rev.* B **43** 4119
[30] Kopf R T, Herman M H, Schnoes M L and Colvard C 1993 *J. Vac. Sci. Technol.* B **11** 813
[31] Contreras-Solorio D A, Velasco V R and García-Moliner F 1993 *Phys. Rev.* B **48** 12 319
[32] Armelles G, Castrillo P, Dominguez P S, González L, Ruiz A, Contreras D A, Velasco V R and García-Moliner F 1993 *J. Physique Coll.* **3** C5 283
[33] Armelles G, Castrillo P, Dominguez P S, González L, Ruiz A, Contreras-Solorio D A, Velasco V R and García-Moliner F 1994 *Phys. Rev.* B **49** 14 020
[34] Vlaev S, Velasco V R and García-Moliner F 1994 *Phys. Rev.* B **50** 4577
[35] Vlaev S, Velasco V R and García-Moliner F 1995 *Phys. Rev.* B **51** 7321
[36] Vlaev S, Velasco V R and García-Moliner F 1995 *Phys. Rev.* B **52** 13 784
[37] Grosso G, Moroni S and Pastori Parravicini G 1989 *Phys. Rev.* B **40** 12 328
[38] Jouanin C, Hallaoui A and Bertho D 1994 *Phys. Rev.* B **50** 1645
[39] Armelles G, Muñoz M C, Velasco V R and García-Moliner F 1990 *Superlatt. Microstruct.* **7** 23